Material modeling of plain concrete

Autor(en): **Chen, Eugene Y.-T. / Schnobrich, William C.**

Objekttyp: **Article**

Zeitschrift: **IABSE reports of the working commissions = Rapports des commissions de travail AIPC = IVBH Berichte der Arbeitskommissionen**

Band (Jahr): **34 (1981)**

PDF erstellt am: **25.04.2024**

Persistenter Link: https://doi.org/10.5169/seals-26878

Material Modeling of Plain Concrete
Un modèle non-linéaire et tridimensionel pour le béton est proposé
Modellbildung für das Verhalten von Beton

EUGENE Y.-T. CHEN and WILLIAM C. SCHNOBRICH
Research Assistant Professor
Department of Civil Engineering,
University of Illinois at Urbana-Champaign
Illinois, USA

SUMMARY
A nonlinear three dimensional material model for plain concrete is proposed. This model consists of a plasticity-based constitutive relation for the quasiductile behavior of concrete; a principal-stress and a principal-strain-based criterion to monitor the initiation of cracks in tension dominated regions as well as cracking due to the poisson effect; a relative-strain-based concept to gauge the cross-crack stress and stiffness transfer; and a strain-based crushing criterion to indicate the local failure of concrete. Some numerical examples to test the proposed model are also included.

RÉSUMÉ
Ce modèle consiste en une relation constitutive pour le comportement quasiductile du béton qui est basée sur la théorie de la plasticité; à l'aide d'un critère exprimé en fonction des contraintes et dilatations principales on peut contrôler le début de la fissuration dûe à la traction ou aux effets de Poisson; un concept basé sur les dilatations relatives permet d'estimer le transfert de contraintes et de rigidité à travers les fissures tandis que la rupture locale du béton est déterminée en fonction d'un écrasement limite. On vérifie le modèle à l'aide de quelques exemples numériques.

ZUSAMMENFASSUNG
Für den Beton wird ein nichtlineares, dreidimensionales Materialmodell vorgeschlagen, welches auf der Plastizitätstheorie basiert. Mit diesem Stoffgesetz wird das quasiduktile Verhalten von Beton beschrieben; ein Hauptspannungs- und ein Hauptdehnungskriterium wird benützt, um den Rissbeginn in Zugzonen, als auch infolge des Poisson-Effekts zu erfassen; ein Konzept, welches auf Relativdehnungen beruht, erlaubt die Abschätzung der Spannungs- und Steifigkeitsübertragung durch Risse hindurch; und ein auf Stauchungen gegründetes Bruchkriterium beschreibt das örtliche Versagen des Betons. Anhand einiger numerischer Beispiele wird das vorgeschlagene Modell überprüft.

1. INTRODUCTION

Reinforced concrete is by far one of the most commonly used construction materials. This composite material demonstrates a highly nonlinear behavior caused by cracking, crushing, aggregate interlock, bond slip, dowel action, shrinkage and creep, etc. Because reinforced concrete involves so many nonlinear phenomena interacting with one another, the formulation of a "complete" analytical model is very difficult. Consequently, most of the research related to behavior of reinforced concrete structures has been of an experimental nature. Within the past several years there has emerged however an attempt to supplement the experimental effort with numerical analysis. Activity has grown quite rapidly in this endeavor and much progress has been reported [3, 4, 16, 17]. Among the various analytical tools available the computer based finite element method has been accepted as the most powerful one. However, even with the large scale general purpose computer programs accessible today, it is felt that the incompleteness of material models for reinforced concrete is still the biggest limiting factor to the current capacity of structural analysis. The focus of this paper is cast on the three dimensional nonlinear constitutive relations and failure criterion for plain concrete subjected to short term monotonic loading.

2. MATERIAL CHARACTERISTICS AND IDEALIZATION

Concrete exhibits an intrinsic brittleness (low tensile strength) through the formation of cracks. Microcracks exist even before any mechanical load is applied. Both the strength and stiffness of concrete are largely determined by the details of the microcracking process [7, 9]. Concrete, when subjected to multiaxial compression, will exhibit an increasing "pseudo-plastic" behavior as the hydrostatic pressure increases. This "pseudo-plastic" behavior phenomenologically resembles the plastic response experienced by ductile metals. The difference between the two types of materials is that in ductile metals plastic flow is caused by lattice dislocation due to material imperfection, while in concrete it is the result of microcracking.

Based on experimental observations, the general response of concrete can be classified into two stages. A "quasi-ductile" stage characterized by "pseudo-plastic" behavior, followed by a brittle failure herein referred to as "crushing". Microcracking plays an important role in the first stage. The growth and the later bridgement of microcracks into a continuous pattern directly leads to the final crushing of concrete. Depending on the loading, the length of the first, the quasi-ductile, stage will vary. With unreinforced concrete if the loading involves a dominant or significant tension the material is considered failed as soon as cracking occurs.

Because concrete resembles partly the ductile metal behavior and partly the brittle ceramic behavior, an elastic plastic fracture material idealization is adopted in this study to delineate the observed (phenomelogical) time independent behavior of concrete.

3. MATHEMATICAL PRELIMINARIES

In general, the stress tensor defining the state of stress at a point can be depicted as a point in a nine dimensional Eculidean stress space. This stress tensor can be decomposed into two parts; the hydrostatic stress part, σ_m, and the deviatoric stress part, S_{ij}, as follows:

$$\sigma_{ij} = S_{ij} + \sigma_m \cdot \delta_{ij} \tag{1}$$

where $\sigma_m = \frac{1}{3}\sigma_{kk}$; and $S_{ij} = \sigma_{ij} - \sigma_m \cdot \delta_{ij}$ in which δ_{ij} is the Kronecker delta.

Because the stress tensor is real and symmetrical (in the absence of body and surface couples), a set of three orthogonal principal stress directions exist. These directions can be used as a reference frame to describe the same stress point in that space but now involving only three coordinates. A convenient alternative to this principal stress reference is the Haigh-Westergard coordinate system. The geometric representation of these two systems in three dimensional Euclidean stress space is given in Fig. 1 where

$$\xi = |\overline{ON}| = \frac{I_1}{\sqrt{3}}$$

$$\rho = |\overline{NP}| = \sqrt{2J_2}$$

$$\theta_1 = \frac{1}{3}\cos^{-1}(y), \quad 0 \leq \theta_1 \leq 60^o \tag{2}$$

$$\theta_2 = \frac{1}{3}\cos^{-1}(-y), \quad 0 \leq \theta_2 \leq 60^o$$

$$y = \frac{3\sqrt{3}}{2}\,\frac{J_3}{J_2^{3/2}}$$

$$I_1 = \sigma_{kk} = 3\sigma_m$$

$$J_2 = \frac{1}{2} S_{ij} \cdot S_{ij}$$

$$J_3 = \frac{1}{3} S_{ij} \cdot S_{jk} \cdot S_{ki}$$

In these equations is the projection of the stress tensor on the hydrostatic axis, $\underline{n} = 1/\sqrt{3}(1,1,1)$; ρ is the projection of the stress tensor on the deviatoric plane (π-plane); θ_1, and θ_2 are Lode angles (angles of similarity) with $\theta_1 + \theta_2 = 60^o$; I_1 is the first invariant of the stress tensor; and J_2, and J_3 are the second and third invariants of the deviatoric stress tensor. The sign convention used throughout this study is tension (+), compression (-).

4. PLASTICITY IN CONCRETE

In order to apply the traditional incremental theory of plasticity to concrete four things have to be defined apriori: (1) the ultimate strength condition which sets the upper bound of the attainable stresses; (2) the initial yield condition which marks the beginning of plastic flow; (3) the flow rule which relates the plastic strain increments to stress increments; (4) the hardening law which dictates the evaluation of the subsequent yield conditions. Geometrically, the initial and subsequent yield conditions can be represented as different surfaces in stress space analogous to the aforementioned ultimate strength condition (Fig. 2). The initial yield surface is a surface that can only be reached by elastic action. If the straining is continued beyond the current yield surface, a new subsequent yield surface will be developed resulting in some additional plastic flow (microcrack growth in concrete). Upon unloading then reloading, no irrecoverable deformation will occur until this new subsequent yield surface is reached.

Test results indicate that the maximum attainable stresses constitute a convex surface in stress space. The shape of this surface resembles that of a Mohr-Coulomb surface. In the principal stress space this ultimate strength surface follows closely that of a smooth six-fold symmetric conical shape with convexly curved meridians which do not intersect the negative hydrostatic axis. This six-fold symmetry supports the macroscopic isotropy assumption for concrete. Because of the symmetry only a 60^{o} spanned region bounded by the tensile meridian, ρ_t, and the compressive meridian, ρ_c, is essential in defining the ultimate strength surface. If $(\sigma_1, \sigma_2, \sigma_3)$ are principal stresses in descending order, then the tensile meridian, ρ_t, corresponds to the stress condition that $\sigma_1 > \sigma_2 = \sigma_3$; while the compressive meridian, ρ_c, corresponds to that of $\sigma_1 = \sigma_2 > \sigma_3$. Once these two bounding meridians are defined, intermediate meridians, ρ, which correspond to various stress combinations can be interpolated using the Lode angle.

Based on test results [2, 8, 14] and least square fitting [12], the tensile and compressive meridians can be expressed as functions of the hydrostatic parameter, ξ:

$$\frac{\rho_t}{f'_c} = -6.4899 + 2.9458\sqrt{5.0343 - \xi/|f'_c|}$$
$$\frac{\rho_c}{f'_c} = -3.6199 + 2.9458\sqrt{1.6907 - \xi/|f'_c|} \qquad (3)$$

in which f'_c is the uniaxial compressive strength of concrete (Fig. 3). Both the tensile and compressive meridians intersect the positive hydrostatic axis at $\xi/f'_c = -0.18064$. It means that concrete cracks under hydrostatic tension when $\xi/f'_c = -0.18064$.

By fitting hyperbolas to the corners of the Mohr-Coulomb type failure locus on the deviatoric plane (Fig. 4), the ultimate strength surface can be expressed as

$$f(\sigma_{ij}) = \sqrt{2J_2} - [(1-S^2\theta_1^2)\,\rho_1 + S^2\theta_1^2\,\rho_2] = 0 \qquad (4)$$

where

$$S = \frac{1}{60^o} \text{ (or } \frac{3}{\pi})$$

$$\rho_1 = \frac{(1+m) \cdot \rho_t \cdot \cos\theta_1 - \sqrt{(1+2m)\cdot\rho_t^2\cdot\sin^2\theta_1\cdot\cot^2\alpha + m^2\cdot\rho_t^2\cdot\cos^2\theta_1}}{\{\cos^2\theta_1 - \sin^2\theta_1 \cdot \cot^2\alpha\}}$$

$$\rho_2 = \frac{(1+m) \cdot \rho_c \cdot \cos\theta_2 - \sqrt{(1+2m)\cdot\rho_c^2\cdot\sin^2\theta_2\cdot\cot^2\beta + m^2\cdot\rho_c^2\cdot\cos^2\theta_2}}{\{\cos^2\theta_2 - \sin^2\theta_2 \cdot \cot^2\beta\}}$$

in which

$$R_\rho = \frac{\rho_t}{\rho_c}$$

$$\cot\alpha = \frac{2}{\sqrt{3}} (R_\rho - 0.5)$$

$$\cot\beta = \frac{2}{\sqrt{3}} (\frac{1}{R_\rho} - 0.5)$$

When applied to the biaxial case, the proposed ultimate strength criterion in Eq. 4 correlates well with the standard test results of Kupfer et al. [8] (Fig. 5).

It is convenient to assume that the initial and subsequent yield conditions have the same functional form as the ultimate strength criterion defined in Eq. 4

$$f(\sigma_{ij},\omega) = \sqrt{2J_2} - \omega[(1-S^2\theta_1^2)\ \rho_1 + S^2\theta_1^2\ \rho_2] = 0 \qquad (5)$$

where w is now added as the hardening parameter to monitor the change of the yield condition. For concrete the initial value for w, which corresponds to the initial yielding, varies in the range of 0.3 to 0.5. The ultimate value for w which corresponds to the ultimate strength is 1. The values in between the initial and the ultimate cases correspond to various intermediate yield conditions.

In this study it was found that with the selected surface an associated flow rule (Fig. 6) does not hold for the whole spectrum of the response of concrete. An equivalent nonassociated flow rule is thus gradually mobilized as the stress level increases. The equivalent nonassociated flow rule is proposed through the use of a piecewise continuous yield surface together with its associated flow rule (Fig. 7). By properly adjusting the angle as yielding progresses, in other words tuning the inclination of each infinitesimal piece on the yield surface, an overstiffening effect can be assuaged while maintaining symmetry in the elastic-plastic constitutive relations. The modified ϕ angle designated by ϕ^* is defined as

$$\phi^* = \phi \cdot [(1-S^2\theta_1^2) + (S^2\theta_1^2) \cdot \phi_\xi] \qquad (6)$$

in which

$$\phi = \tan^{-1}\left(\frac{\partial f}{\partial \xi}\right) \qquad \text{and} \qquad \phi_\xi = \phi_w \cdot \left[1 - \frac{1}{1 + \frac{1}{\sigma_h}}\right]$$

with

$$\sigma_h = \frac{\xi}{f'_c} + 0.18064$$

and

$$\phi_w = 1, \text{ when } 0 \leq w \leq w_c$$

$$= 1 - \frac{w - w_c}{1 - w_c}, \text{ when } w_c \leq w \leq 1$$

where w_c is the hardening parameter at which an overstiffening effect becomes significant. Generally this corresponds to the onset of mortar cracking at $w_c = 0.7$ to 0.8.

Based on the modified ϕ angle, the outward normals of the hypothesized piecewise continuous yield surface can be written as

$$a_{ij} = (\tan \phi^*) \cdot \left(\frac{d\xi}{d\sigma_{ij}}\right) + \frac{\partial f}{\partial J_2} \cdot \left(\frac{dJ_2}{d\sigma_{ij}}\right) + \frac{\partial f}{\partial J_3} \cdot \left(\frac{dJ_3}{d\sigma_{ij}}\right) \tag{7}$$

Because this paper is concerned only with short-term monotonic loading, an isotropic hardening law is used.

If we assume elastic unloading behavior of concrete together with the associated flow rule and the consistency condition (neglecting the viscosity effect) [10], the incremental elastic plastic constitutive relation can be expressed as

$$d\sigma_{ij} = \left[D_{ijkl} - \frac{D_{ijmn} \cdot a_{mn} \cdot a_{rs} \cdot D_{rskl}}{Y + a_{mn} \cdot D_{mnrs} \cdot a_{rs}}\right] \cdot d\varepsilon_{kl}$$

$$= D^{ep}_{ijkl} \cdot d\varepsilon_{kl} \tag{8}$$

where D_{ijkl}, D_{ijmn}, D_{rskl}, D_{mnrs} are elastic constitutive coefficients; D^{ep}_{ijkl} are elastic-plastic constitutive coefficients; a_{mn}, a_{rs} are the outward normals to the yield surface; and $Y = -\frac{\partial f}{\partial \omega}\frac{d\omega}{d\lambda}$ with $d\lambda$ the instantaneous constant of proportionality used in the flow rule.

5. CRACK MODELING IN CONCRETE

In this study the smeared crack approach is adopted. The advantage of using this approach lies in the fact that it avoids the constant changing of structure topology. The smeared crack representation, which corresponds to an averaging (smoothing) procedure of local discontinuities, allows an equivalent continuum treatment with localized material anisotropy. It simplifies the solution algorithms substantially. Also, it fits well into the approximate nature of the finite element method with C_o-continuity of displacement and bounded nonsingular strain and stress fields. However, it should be noted

that the smeared crack representation tends to diffuse the cracking system. Consequently, no single crack can dominate the behavior.

Experimental observation from different sources all indicate that maximum tensile deformation measured by the maximum tensile strain component is a dominant parameter in predicting brittle fracture of concrete [1]. The Poisson effect may cause some inconsistency when this so called "principal strain criterion" is subjected to multiaxial stress conditions [13]. Nevertheless, the simplicity of this criterion and the fact that it is used only for crack initiation in completely intact concrete make its use feasible. Consequently, it is assumed that the plane of cracking in concrete is normal to the direction of maximum tensile strain component.

Because an orthogonal set of opening cracks is enforced in this study, the direction for any subsequent crack formed in the uncracked subspace following an initial crack is thus fixed. A stress-based new crack initiation criterion is used. This stress-based criterion is very similar to the commonly used "principal stress criterion", except that the direction of this potential crack is pre-defined.

6. RELATIVE STRAIN ACROSS THE CRACK

In the framework of continuum mechanics, a crack may be looked upon as a separation of two neighboring material particles. Upon cracking certain components of displacements will become discontinuous, which implies "relative movement" between the two sides of the crack surface. Because displacements and strains are related through kinematic equations, it is conceivable within a continuum treatment to assume that a set of relative strains exist which represents the relative movement across the crack. As a matter of fact, these "relative strain" quantities are what have been measured across a crack in the experiments through the use of mechanical strain gauges.

In the equivalent continuum treatment of cracked concrete (smeared crack approach), the "relative strain" can be defined as the elastic portion of the corresponding total strain. Before cracking occurs a complete bonding exists between two neighboring particles. It is this bonding that allows them to deform or to be strained together. Once cracking starts, a separation which implies relative movements between these two neighboring particles will occur. These relative movements can be interpreted as a relaxation of the deformation (straining) of one particle with respect to the other. Since the plastic portion of deformation (straining) is nonrecoverable, it is logical to assume that the elastic portion must account for the relaxation and hence the corresponding relative movements. This "relative strain" is more a mathematical than physical parameter. It is used to gauge the local cross-crack stress and stiffness transfer [5].

7. CROSS-CRACK CONSTITUTIVE RELATIONS

Let n, s and t be a set of righthanded orthogonal coordinate directions with n normal and s, t tangential to the cracked surface.

The 3-D cross-crack constitutive relations in terms of stress and relative strain components across the crack, can be described in a matrix form as follows

$$\begin{Bmatrix} \sigma_n \\ \sigma_s \\ \sigma_t \end{Bmatrix} = \begin{bmatrix} k_{nn} & k_{ns} & k_{nt} \\ k_{sn} & k_{ss} & k_{st} \\ k_{tn} & k_{ts} & k_{tt} \end{bmatrix} \begin{Bmatrix} \tilde{\varepsilon}_n \\ \tilde{\varepsilon}_s \\ \tilde{\varepsilon}_t \end{Bmatrix} \tag{9}$$

in which K_{nn} is the cross-crack normal stiffness coefficient; K_{ss}, K_{tt} are the cross-crack shear stiffness coefficients; K_{sn}, K_{tn} are the cross-crack coupled shear stiffness coefficients; K_{ns}, K_{nt} are the cross-crack dilatant-contractant stiffness coefficients; and K_{st}, K_{ts} are the cross-crack cross-shear stiffness coefficients.

Upon replacing the stress and relative strain components in Eq. 9 by the corresponding stress and relative strain increments a set of incremental cross-crack constitutive relations are thus obtained. The assumption in doing so is that the interface stiffness coefficients are path independent in the sense that they are functions only of the current total stresses and the accumulated relative strains.

The stiffness coefficients in Eq. 9 are generally unsymmetrical. Because a symmetric matrix is always desirable from a programming point of view, Eq. 9 is modified so that a symmetric constitutive matrix is achieved as shown in Eq. 10.

$$\begin{Bmatrix} \Delta\sigma_n \\ \Delta\sigma_s \\ \Delta\sigma_t \end{Bmatrix} = \begin{bmatrix} k_{nn} & \frac{1}{2}(k_{ns}+k_{sn}) & \frac{1}{2}(k_{nt}+k_{tn}) \\ \frac{1}{2}(k_{ns}+k_{sn}) & k_{ss} & \frac{1}{2}(k_{st}+k_{ts}) \\ \frac{1}{2}(k_{nt}+k_{tn}) & \frac{1}{2}(k_{st}+k_{ts}) & k_{tt} \end{bmatrix} \begin{Bmatrix} \Delta\tilde{\varepsilon} \\ \Delta\tilde{\varepsilon} \\ \Delta\tilde{\varepsilon} \end{Bmatrix} \tag{10}$$

In the following section, the cross-crack constitutive relations defined here are referred to as the "CSST Model."

8. POST-CRACKING MODEL FOR CONCRETE

Once cracking occurs, the material coordinate system is locally fixed due to the crack introduced anisotropy. Cracks in orthogonal directions can occur simultaneously or subsequently whenever the crack initiation criterion is met in an intact subspace of concrete. This allows concrete to have multi-directional cracking. Upon cracking, Eq. 8 written in the current

principal strain directions (material coordinate directions) needs to be modified to account for the existence of cracks and to simulate the post-cracking behavior of concrete. For this purpose, the CSST model is used, while the constitutive relations for the intact concrete are still enforced in the unracked subspace of concrete.

In this study a gradual stress releasing is implemented through the gradual activation of the CSST model after cracking occurs. This is done by using stress-level-dependent activating factors for the CSST stiffness coefficients when averaging them with those coefficients in Eq. 8 to obtain the final elastic-plastic-fracture stiffness. Letting the numbers 1, 2, 3 represent the current material coordinate directions, the fracture constitutive relations can be written as follows

$$\begin{Bmatrix} \sigma_{11} \\ \sigma_{12} \\ \sigma_{13} \\ \sigma_{21} \\ \sigma_{22} \\ \sigma_{23} \\ \sigma_{31} \\ \sigma_{32} \\ \sigma_{33} \end{Bmatrix} = \begin{bmatrix} W_1 \cdot (^{CSST}_{Model}) & 0 & 0 \\ 0 & W_2 \cdot (^{CSST}_{Model}) & 0 \\ 0 & 0 & W_3 \cdot (^{CSST}_{Model}) \end{bmatrix} \begin{Bmatrix} \tilde{\varepsilon}_{11} \\ \tilde{\varepsilon}_{12} \\ \tilde{\varepsilon}_{13} \\ \tilde{\varepsilon}_{21} \\ \tilde{\varepsilon}_{22} \\ \tilde{\varepsilon}_{23} \\ \tilde{\varepsilon}_{31} \\ \varepsilon_{32} \\ \varepsilon_{33} \end{Bmatrix} \qquad (11)$$

The activating factors, W_i, i=1,2,3, are defined as follows: $W_i = 0$ if there is no active crack normal to the i^{th} direction; otherwise

$$W_i = \frac{1}{(1-\omega)^n} \qquad (12)$$

where w is the current hardening parameter; and n is a curve fitting parameter. Multiplying the stiffness coefficients in the CSST model with a factor of $(\tilde{\varepsilon}_{ij} / \varepsilon_{ij})$ where $\tilde{\varepsilon}_{ij}$ and ε_{ij} are accumulated relative strains and total strains respectively. Equation 11 can be written in tensor notation as

$$\sigma_{ij} = W \cdot D^f_{ijkl} \cdot \varepsilon_{kl} \qquad (13)$$

From Eq. 13 the "path independent" incremental fracture constitutive relations can be written as

$$\Delta\sigma_{ij} = W \cdot D^f_{ijkl} \cdot \Delta\varepsilon_{kl} \qquad (14)$$

Combining Eqs. 8 and 14 under the current local material coordinate system, we

get

$$\Delta\sigma_{ij} = \frac{1}{1+W} \cdot [D^{ep}_{ijkl} + W \cdot D^{f}_{ijkl}] \cdot \Delta\varepsilon_{kl} = D^{epf}_{ijkl} \cdot \Delta\varepsilon_{kl} \tag{15}$$

where D^{epf}_{ijkl} are the current elastic-plastic-fracture stiffness coefficients.

In general the D^{epf}_{ijkl} are not symmetric, because the fracture destroys the continuity originally existing in the intact material. However, in this study an equivalent continuum mechanics approach is used which approximates the fracture effect by changing the material properties. Hence it is proposed to symmetrize the elastic-plastic-fracture stiffness coefficients by letting

$$D^{epf}_{ijkl} = D^{epf}_{jikl} = D^{epf}_{ijlk} = D^{epf}_{klij} = (D^{epf}_{ijkl} + D^{epf}_{jikl} + D^{epf}_{ijlk} + D^{epf}_{klij})/4 \tag{16}$$

In order to be consistent with other parts of the structure, D^{epf}_{ijkl} have to be transformed from their local material coordinate system into the predetermined structural coordinate system.

9. STRAIN-BASED FAILURE CRITERION

The failure criterion prescribes the stress and/or strain condition at which the concrete loses all of its stiffness as well as load carrying capacity. In this study a strain-based failure criterion is adopted. Concrete is considered crushed when

$$\frac{\varepsilon_{eq.}}{\varepsilon_0} \geq R_\varepsilon \tag{17}$$

in which $\varepsilon_{eq.}$ is the equivalent uniaxial strain defined in Eq. 18; ε_o is defined in Eq. 22; and R_ε is defined in Eq. 21 (Fig. 8).

10. EQUIVALENT UNIAXIAL STRESS AND STRAIN

In order to evaluate the parameter Y in Eq. 8 as plastification occurs, the plastic hardening modulus, H, has to be calibrated apriori. A commonly used approach in calculating H is to deduce from the multidimensional condition a pair of quantities, the equivalent uniaxial stress, $\sigma_{eq.}$, and the strain $\varepsilon_{eq.}$. By doing so the well documented uniaxial test results can be generalized and extrapolated. In this study it was found that concrete behavior is very sensitive to the use of an equivalent uniaxial strain once cracks have occurred. This is because the fracture introduced softening effect damages the consistency and integrity of the equivalent uniaxial stress-strain approach used in the plasticity theory. With this drawback in mind, the following definition for the equivalent uniaxial strain is used in this study. It is made up of an elastic part, $\varepsilon^e_{eq.}$, and a plastic part, $\varepsilon^p_{eq.}$.

$$\varepsilon_{eq.} = \varepsilon^e_{eq.} + \varepsilon^p_{eq.} = \frac{\omega . |f'_c|}{E} + \varepsilon^p_{eq.} \tag{18}$$

where w is the current hardening parameter defined as $w = \sigma_{eq.} / |\sigma_o|$; f'_c and

E are the uniaxial compressive strength and the initial modulus of elasticity respectively; and $\varepsilon^{p}_{eq.}$ is the accumulated equivalent uniaxial plastic strain defined in Eq. 23.

In this study the generalized uniaxial compressive stress-strain relationship of Saenz is used [15], Fig. 8.

$$\sigma_{eq.} = \frac{E \cdot \varepsilon_{eq.}}{1 + (R+R_E-2)\left(\frac{\varepsilon_{eq.}}{\varepsilon_0}\right) - (2R-1)\left(\frac{\varepsilon_{eq.}}{\varepsilon_0}\right)^2 + R\left(\frac{\varepsilon_{eq.}}{\varepsilon_0}\right)^3} \tag{19}$$

The equivalent uniaxial tangent modulus is

$$E_t = \frac{d\sigma_{eq.}}{d\varepsilon_{eq.}} = \frac{E \cdot \left[1+(2R-1)\left(\frac{\varepsilon_{eq.}}{\varepsilon_0}\right)^2 - 2R\left(\frac{\varepsilon_{eq.}}{\varepsilon_0}\right)^3\right]}{\left[1+(R+R_E-2)\left(\frac{\varepsilon_{eq.}}{\varepsilon_0}\right) - (2R-1)\left(\frac{\varepsilon_{eq.}}{\varepsilon_0}\right)^2 + R\left(\frac{\varepsilon_{eq.}}{\varepsilon_0}\right)^3\right]^2} \tag{20}$$

in which σ_o and ε_o are the peak strength and corresponding strain under the current stress combination, and ε_f and σ_f are the maximum strain and corresponding stress under the current stress combination. The remaining terms in Eqs. 19 and 20 are defined by the following equations:

$$\begin{aligned} E_S &= \frac{\sigma_0}{\varepsilon_0} \\ R_E &= \frac{E}{E_S} \\ R_\sigma &= \frac{\sigma_0}{\sigma_f} \\ R_\varepsilon &= \frac{\varepsilon_f}{\varepsilon_0} \\ R &= \frac{R_E(R_\sigma-1)}{(R_\varepsilon-1)^2} - \frac{1}{R_\varepsilon} \end{aligned} \tag{21}$$

In order to find σ_o, ε_o, σ_f and ε_f under the current stress combination, the following algorithm is used.

1) Extend a line from the origin in the stress space through the current stress point until it penetrates the ultimate strength surface. Then calculate its length.

2) Find the ratio, r, between the length just calculated and the length corresponding to the uniaxial compression case.

3) $\sigma_0 = r \cdot f'_c$

4) $\varepsilon_0 = \varepsilon_c \cdot [r \cdot T-(T-1)]$, if $r \geq 1$;

$\varepsilon_0 = \varepsilon_c \cdot [-1.6\, r^3 + 2.25 r^2 + 0.35 r]$, if $r < 1$ (22)

where T is taken to be three in this study; and ε_c is the measured uniaxial compressive strain at f_c.

5) $\sigma_f = \sigma_0 / R_\sigma$

6) $\varepsilon_f = R_\varepsilon \cdot \varepsilon_0$

Due to the lack of strain data the empirical formula proposed by Darwin and Pecknold is used to find ε_o. [Darwin, Pecknold, 1974]. Because it is impossible to define σ_f and ε_f on any rigorous experimental basis. it is assumed that $R_\sigma = 4$ and $R_\varepsilon = 4$ realizing that R_σ and R_ε do not have to be the same. Since σ_o and ε_o are calculated differently, the secant modulus, E_s, is not a constant value but a function of the current stress combination.

If the strain hardening hypothesis is used then $w = w(\varepsilon^P_{eq.})$, where $\varepsilon^P_{eq.}$ is the accumulated equivalent uniaxial plastic strain defined as

$$\varepsilon^P_{eq.} = \int d\varepsilon^P_{eq.} = \int m_p \cdot (d\varepsilon^P_{ij} \cdot d\varepsilon^P_{ij})^{1/2} = \int m_p \cdot d\lambda \cdot (a_{ij} \cdot a_{ij})^{1/2} \tag{23}$$

where $d\varepsilon^P_{ij}$ are the incremental plastic strain; and m_p is the equivalent uniaxial plastic strain scaling factor.

$$m_p = \frac{s_f}{\sqrt{s_f^2+2}} \tag{24}$$

in which

$$s_f = \frac{\sqrt{2}}{\tan(\theta+\phi^*)}$$

$$\theta = \cos^{-1}(\sqrt{2/3})$$

It is noted that for hydrostatic insensitive materials $\phi = \phi^* = 0$ and $m_p = \sqrt{2/3}$

If elastic unloading is assumed, then the plastic hardening modulus, H, can be related to the initial and tangent moduli as follows

$$H = \frac{d\sigma_{eq.}}{d\varepsilon^P_{eq.}} = \frac{E_t}{1-\frac{E_t}{E}} \tag{25}$$

From Eqs. 18, 23 and 25 the parameter Y in Eq. 8 can be determined as

$$Y = -\frac{\partial f}{\partial \omega} \cdot \frac{d\omega}{d\lambda} = -\frac{\partial f}{\partial \omega} \cdot \frac{H}{|\sigma_0|} \cdot m_p \cdot (a_{ij} \cdot a_{ij})^{1/2} \qquad (26)$$

11. NUMERICAL STUDY

The proposed constitutive relations are used to simulate the responses of concrete subjected to uniaxial, biaxial, and triaxial compressive loadings. The test and simulated results are shown in Figs. 9-17.

It was found during the study of triaxial loadings, that the phenomenon which is termed yielding in this study existed even under pure hydrostatic stress. This is due to the inelastic compaction of concrete. In order to obtain reasonable results therefore this presence of "yielding" under hydrostatic stress had to be considered. "Classical" plasticity theory, however, does not allow such nonlinear behavior when the material is in a pure hydrostatic stress state. This finding suggests then that a more general approach when using a plasticity theory for concrete in the future may be one that possesses two yield functions, one for volumetric and one for deviatoric response. These two analytical models should be able to interact with each other, so that the shear dilatation and compaction phenomena observed in experiments can be considered.

12. CONCLUSIONS

The smeared crack representation with material sampling points at the integration points proves to be reliable. This statement is valid if the sampling points are not too far away from each other. Consequently, local irregularities will not be overlooked due to the inherent averaging process. Based on this argument, reduced integration should be used with care. Depending on the real stress distribution, sometimes more integration points are needed simply to describe the crack pattern and hence to monitor the nonlinearized material properties with higher precision.

Having been verified on many occasions, the equivalent uniaxial stress-strain approach in a plasticity theory works well with ductile materials. As for concrete, this approach requires further tuning and generalization in order to better reflect the cracking effect.

The equivalent nonassociated flow rule, using a piecewise continuous yield surface to maintain a symmetrical elastic-plastic constitutive matrix, gives a better uniaxial compressive response of concrete than the associated flow rule would.

The "relative strain" parametrization in handling the cross-crack stress and stiffness transfers is a reasonable approach within the realm of continuum mechanics. Besides being a mathematical quantity the "relative strain" also has its practical implication in the mechanical strain gauge measurement across a crack.

REFERENCES

1. Atan, Y., and Slate, F.O., "Structural Lightweight Concrete Under Biaxial Compression," American Concrete Institute Journal, Proceedings, Vol. 70, No. 3, March, 1973, pp. 182-186.

2. Balmer, G.G., "Shearing Strength of Concrete Under High Triaxial Stress-Computation of Mohrs Envelope as a Curve," Structural Research Laboratory Report No. SP-23, U.S. Dept. of the Interior, Bureau of Reclamation, Washington, D.C., 1949.

3. Bazant, Z.P., Schnobrich, W.C., and Scordelis, A.C., Analisi Delle Strutture in Cemento Armato Mediante Il Metodo Degli Elementi Finiti, Carso di Perfezionamento per Le Costruzioni in Cemento Armato "Fratelli Pesenti," Politecnico Di Milano, Italy, 1978.

4. Bergan, P.G., and Holand, I., "Nonlinear Finite Element Analysis of Concrete Structures," International Conf. on Finite Elements in Nonlinear Mechanics, Stuttgart, Germany, (FRG), Aug.-Sept., 1978.

5. Chen, E.Y-T., and Schnobrich, W.C., "Models for the Post-Cracking Behavior of Plain Concrete under Short Term Monotonic Loading," Symposium on Computational Methods in Nonlinear Structural and Solid Mechanics, Oct. 6-8, 1980, Washington D.C.

6. Darwin, 6.D., and Pecknold, D.A.W., "Inelastic Model for Cyclic Biax Loading of Reinforced Concrete," Civil Engineering Studies, SRS No. 409, University of Illinois, Urbana, Illinois, July, 1974.

7. Hsu, 7.T.T.C., Slate, F.O., Sturman, G.M., and Winter, G., "Microcracking of Plain Concrete and the Shape of the Stress-Strain Curve," American Concrete Institute Journal, Proceedings, Vol. 60, No. 2, Feb., 1963, pp. 219-223.

8. Kupfer, H., Hilsdorf, H.K., and Rusch, H., "Behavior of Concrete Under Biaxial Stresses," American Concrete Institute Journal, Proceedings, Vol. 66, No. 8, Aug., 1966, pp. 656-666.

9. Mindess, S., and Diamond, S., "The Cracking and Fracture of Mortar," ASCE Fall Convention, Hollywood, Florida, Oct., 1980.

10. Nayak, G.C., and Zienkiewicz, O.C., "Elasto-Plastic Stress Analysis A Generalization for Various Constitutive Relations Including Strain Softening," International Journal for Numerical Methods in Engineering, Vol. 5, 1972, pp. 113-135.

11. Nelissen, L.J.M., "Biaxial Testing of Normal Concrete," Heron, the Netherlands, Vol. 18, No. 1, 1972.

12. Ottosen, N.S., "A Failure Criterion for Concrete," Journal of the Engineering Mechanics Division, ASCE, Vol. 103, No. EM4, Aug., 1977, pp. 527-535.

13. Pandit, G.S., discussion of "Structural Lightweight Concrete under Biaxial Compression," by Y. Atan and F.O. Slate, American Concrete Institute Journal, Proceedings, Vol. 70, No. 9, Sept., 1973, pp. 660-661.

14. Richart, F.E., Brandtzaeg, A., and Brown, R.L., "A Study of the Failure of Concrete under Combined Compressive Stresses," Bulletin No. 185, University of Illinois, Engineering

15. Saenz, I.P., discussion of "Equation for the Stress-Strain Curve of Concrete," by P. Desayi and S. Krishnan, American Concrete Institute Journal, Proceeding, Vol. 61, No. 9, Sept., 1964, pp. 1229-1235.

16. Schnobrich, W.C., "Behavior of Reinforced Concrete Structures, Predicted by the Finite Element Method," Computers and Structures, Vol. 7, 1977, pp. 365-376.

17. Scordelis, A.C., "General Report-Basic Problems," IASS Symposium on Nonlinear Behavior of Reinforced Concrete Structures, Darmstadt, Germany (FRG), July, 1978.

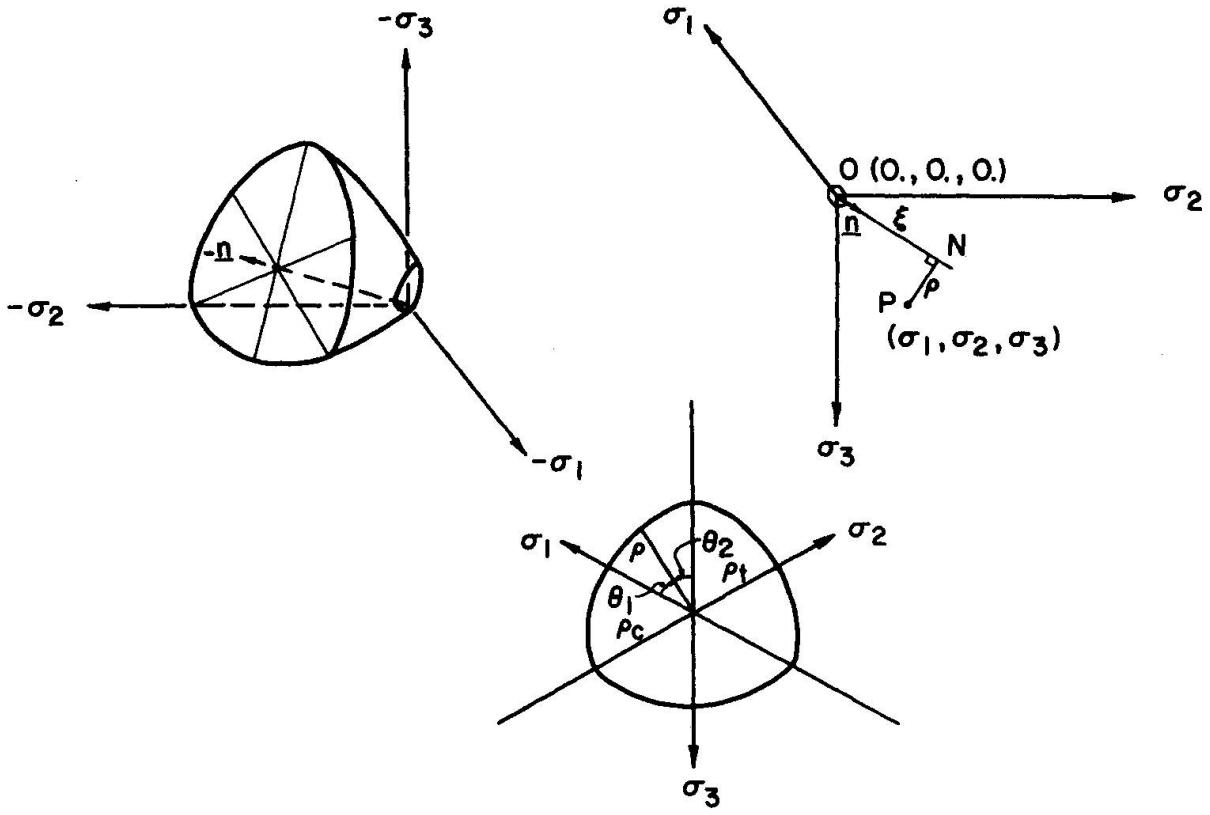

Fig. 1 Haigh-Westergard Coordinate System

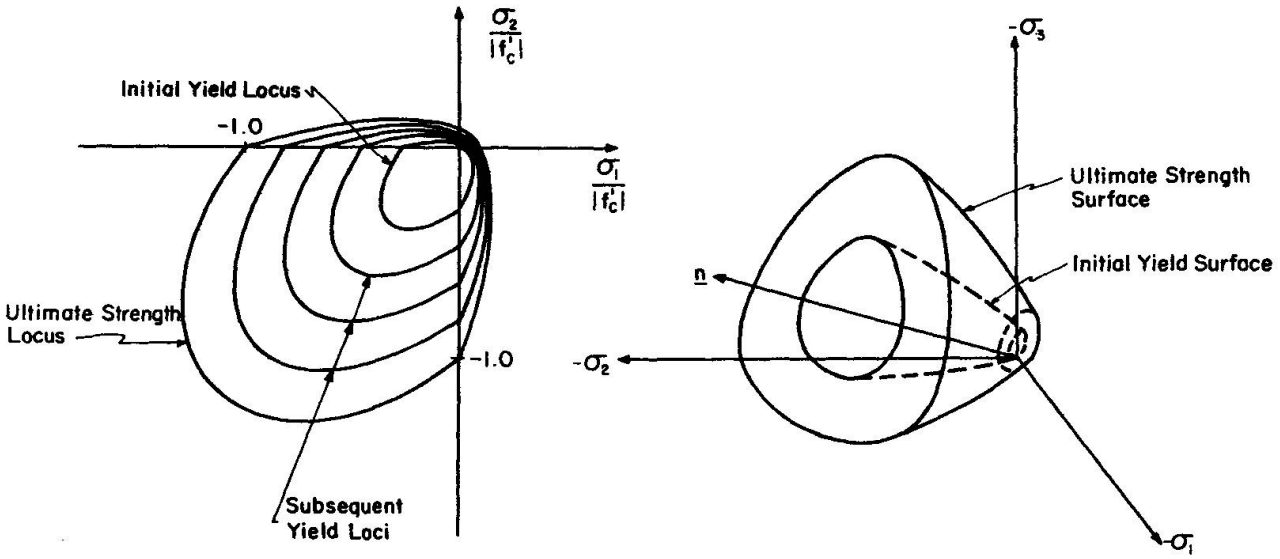

Fig. 2 Yield and Ultimate Strength Surfaces

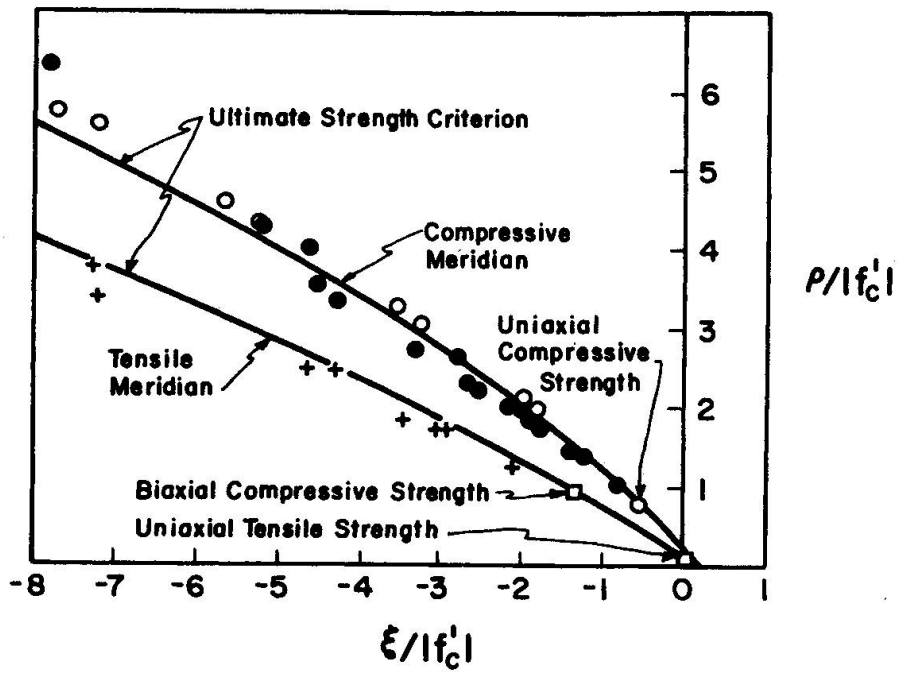

Fig. 3 Tensile and Compressive Meridians

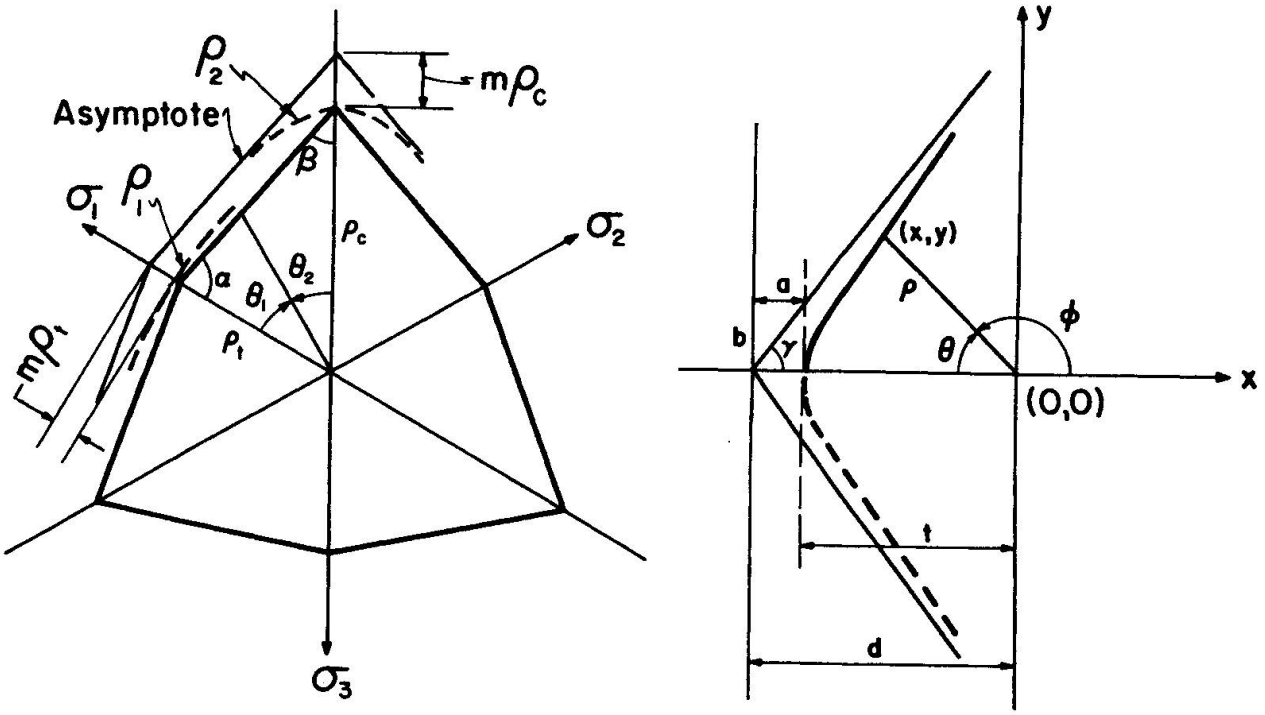

Fig. 4 Hyperbola Fitting

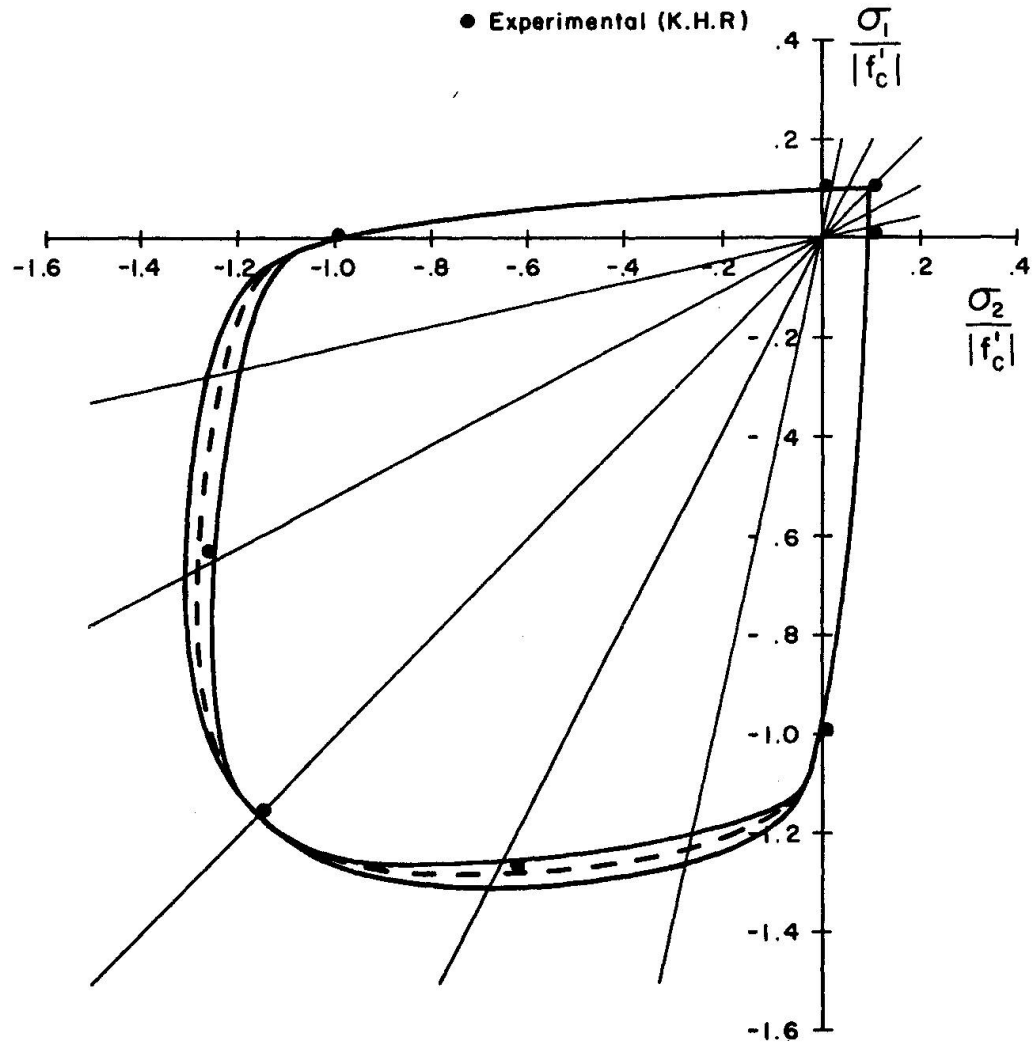

Fig. 5 Biaxial Tests of Kupfer et al

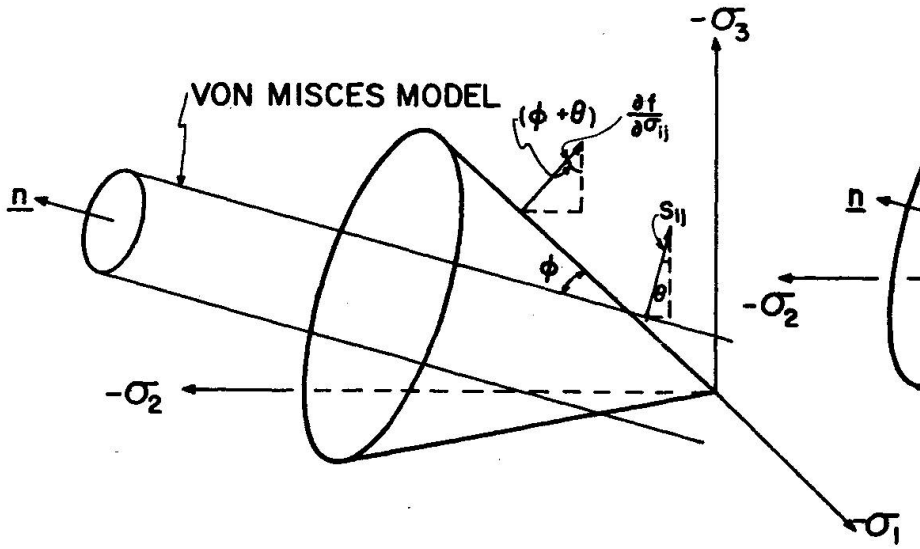

Fig. 6 Normals to the Yield Surfaces

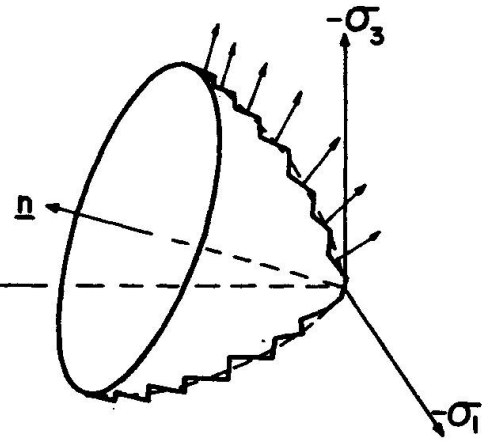

Fig. 7 Piecewise Continuous Yield Surface

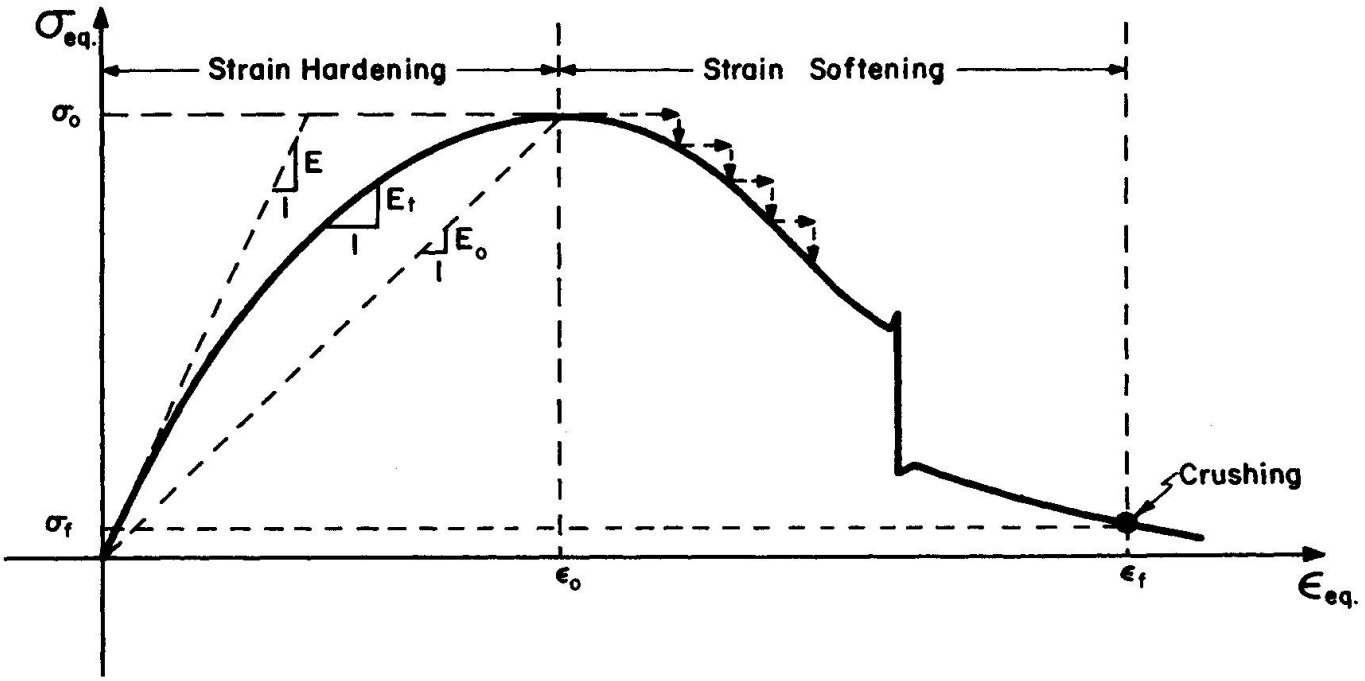

Fig. 8 Uniaxial Stress-Strain Curve of Concrete

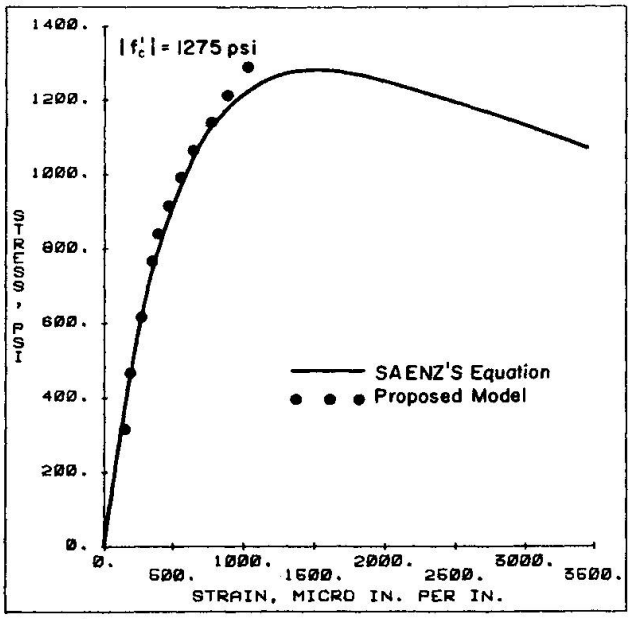

Fig. 9 Uniaxial Compression of Plain Concrete, $|f'_c|$ = 1275 psi

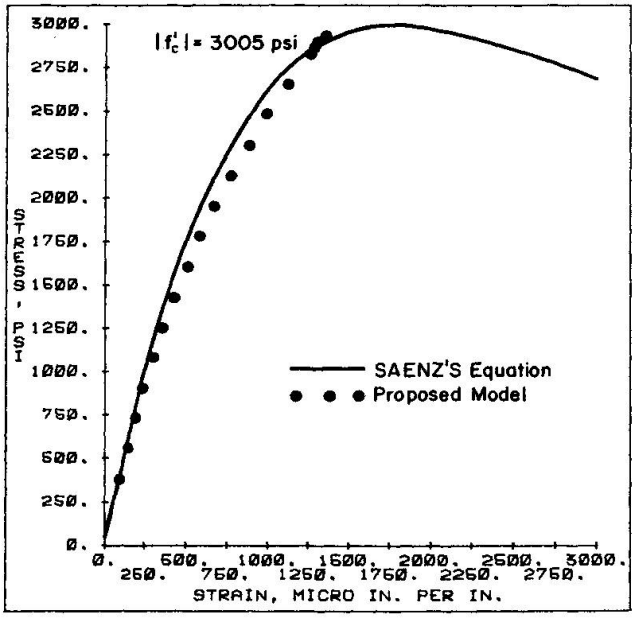

Fig. 10 Uniaxial Compression of Plain Concrete, $|f'_c|$ = 3005 psi

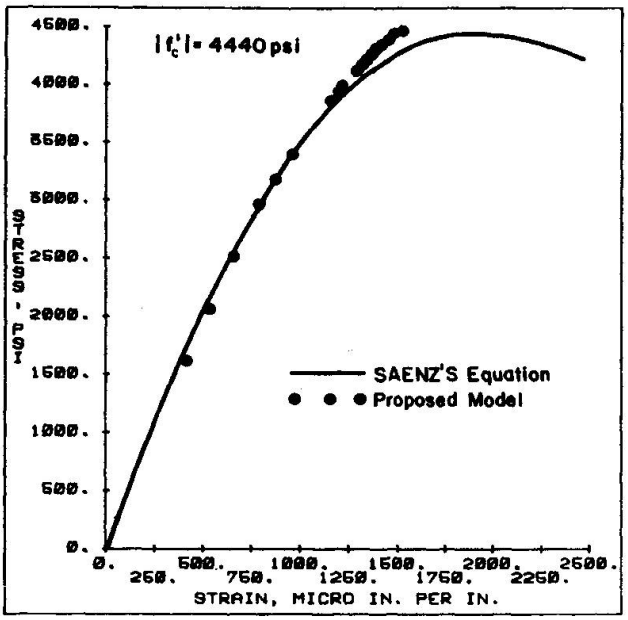

Fig. 11 Uniaxial Compression of Plain Concrete, $|f'_c| = 4440$ psi

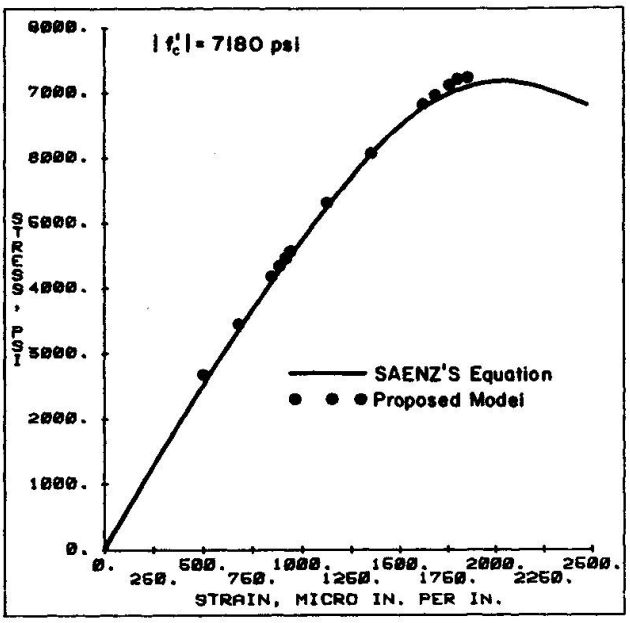

Fig. 12 Uniaxial Compression of Plain Concrete, $|f'_c| = 7180$ psi

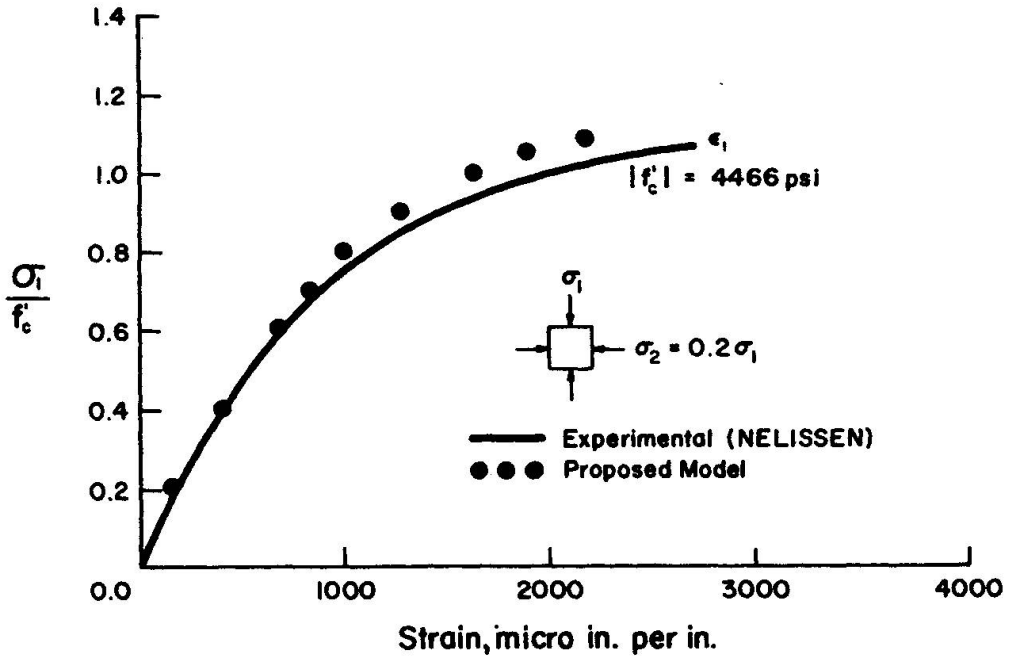

Fig. 13 Biaxial Compression of Plain Concrete, $\sigma_2 = 0.2\sigma_1$

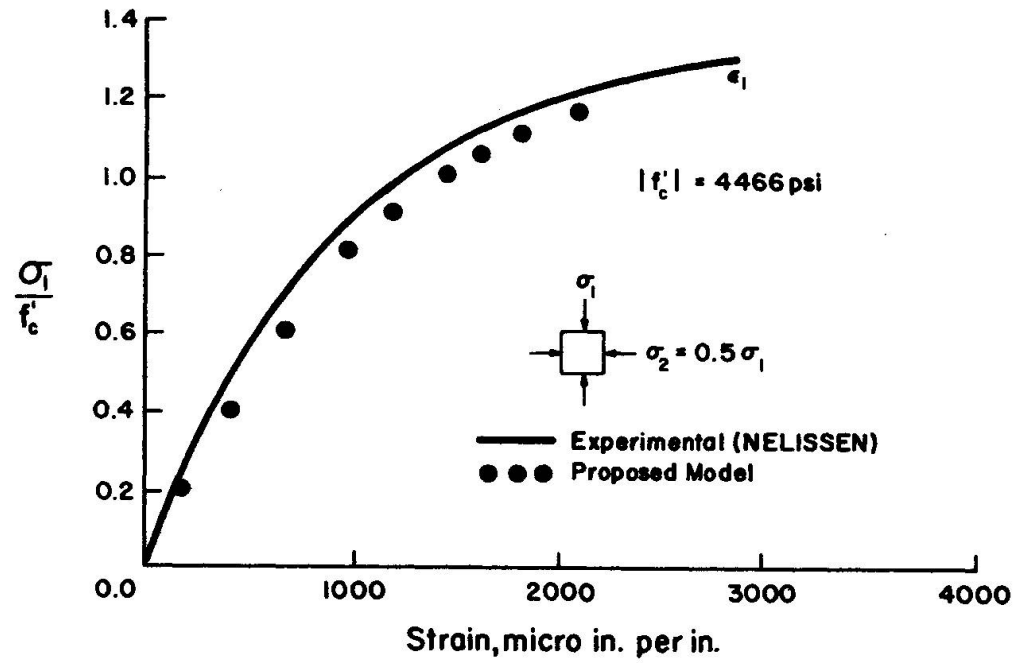

Fig. 14 Biaxial Compression of Plain Concrete, $\sigma_2 = 0.5\sigma_1$

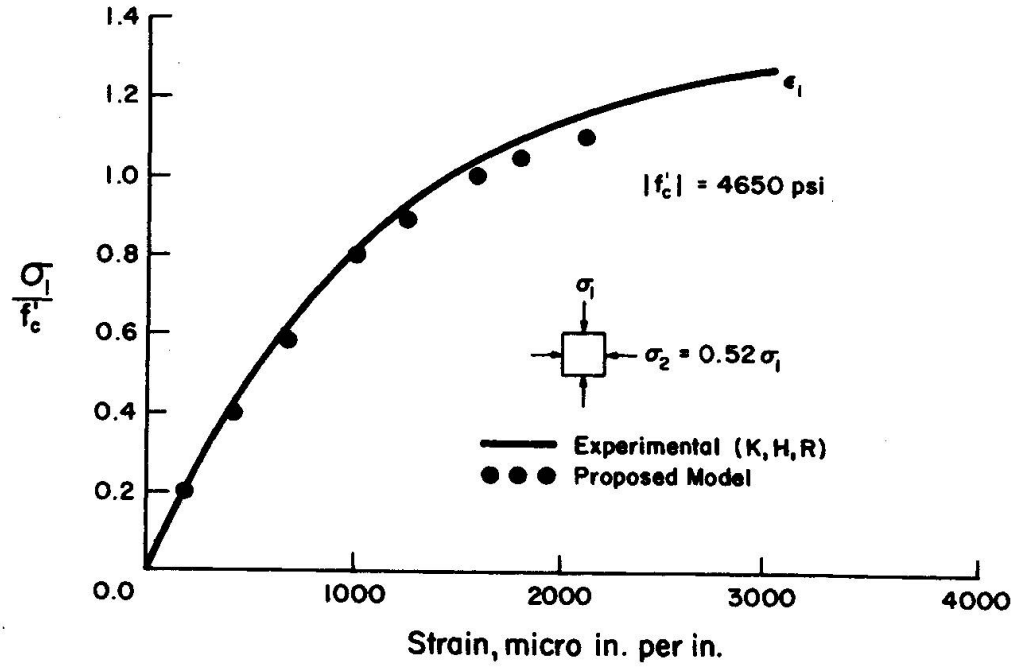

Fig. 15 Biaxial Compression of Plain Concrete, $\sigma_2 = 0.52\sigma_1$

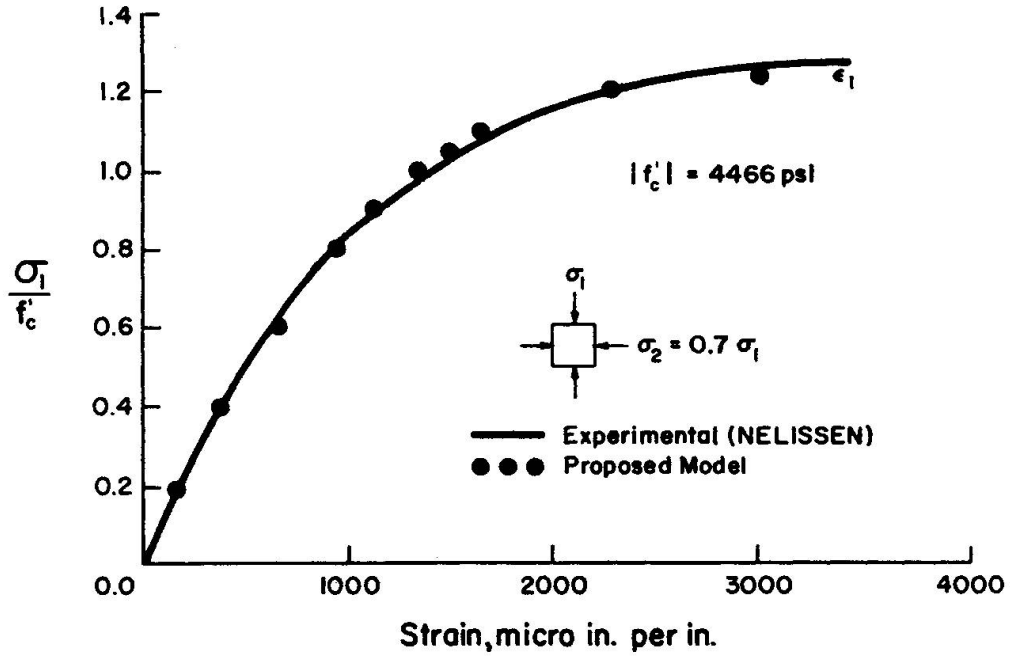

Fig. 16 Biaxial Compression of Plain Concrete, $\sigma_2 = 0.7\sigma_1$

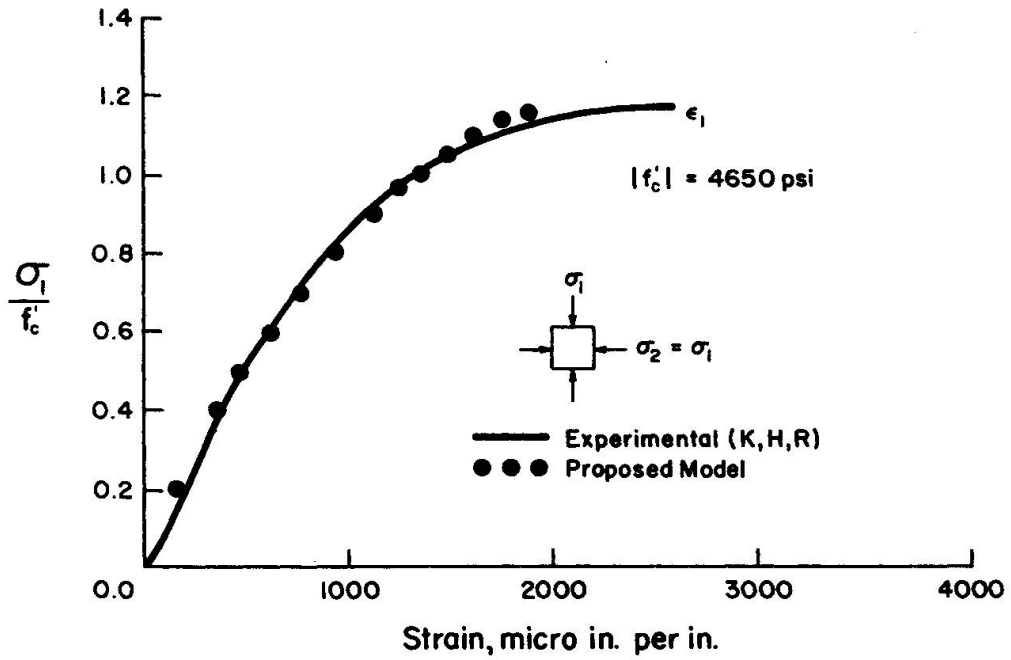

Fig. 17 Biaxial Compression of Plain Concrete, $\sigma_1 = \sigma_2$